NANOSYSTEMS:
PHYSICS, CHEMISTRY, MATHEMATICS

Original article

Almjasheva O.V., et al. *Nanosystems: Phys. Chem. Math.*, 2026, **17** (2), 210–217.
http://nanojournal.ifmo.ru
DOI 10.17586/2220-8054-2026-17-2-210-217

The role of dehydration-hydration in the formation of nanoparticles with a chrysotile structure during hydrothermal treatment of $Mg_{1-x}Ni_x(OH)_2$–SiO_2–H_2O(NaOH) systems

Oksana V. Almjasheva[1,2], Maria E. Kurguzkina[1], Victor V. Gusarov[1]

[1]NRC "Kurchatov Institute" – PNPI – IChS, Russia

[2]Saint-Petersburg Electrotechnical University, Russia

Corresponding author: Almjasheva O.V., almjasheva@mail.ru

ABSTRACT A thermodynamic analysis of hydroxide transformations in the $Mg_{1-x}Ni_x(OH)_2 – SiO_2 – H_2O$ system during the hydrothermal synthesis of nanotubular particles with a chrysotile structure has revealed the decisive role of the dehydration of initial reagents and the subsequent re-formation of hydroxides during hydrothermal treatment of reagents on the composition and morphological parameters of the target product. Depending on the composition of the hydroxide reagent and the *T–P* conditions in the reaction zone, three regions have been identified where the formation mechanism of nanotubular particles with a chrysotile structure changes dramatically. This is the direct cause of the non-monotonic dependence of the Mg/Ni ratio and the dimensional parameters of the $(Mg_{1-x}Ni_x)_3Si_2O_5(OH)_4$ nanotubes on the Mg/Ni ratio in the initial hydroxide.

KEYWORDS solid solutions, hydroxides, oxides, chrysotile, nanotubes, hydrothermal synthesis, thermodynamic calculations

ACKNOWLEDGEMENTS The work was supported by the Russian Science Foundation (RSF) project No. 24-13-00445.

FOR CITATION Almjasheva O.V., Kurguzkina M.E., Gusarov V.V. The role of dehydration-hydration in the formation of nanoparticles with a chrysotile structure during hydrothermal treatment of $Mg_{1-x}Ni_x(OH)_2$–SiO_2–H_2O(NaOH) systems. *Nanosystems: Phys. Chem. Math.*, 2026, **17** (2), 210–217.

1. Introduction

The hydrothermal formation of hydrosilicate nanotubes with a chrysotile structure, characterized by the general formula $Me_3Si_2O_5(OH)_4$, where Me is typically Mg, which can be partially or completely substituted by atoms such as Fe, Co, Ni, etc., has revealed a number of significant differences compared to the formation of oxide and hydroxide nanoparticles of other compositions and morphologies. For instance, while the hydrothermal synthesis of many simple and complex oxides and hydroxides can yield nanoparticles with a relatively narrow size distribution [1–7], the scientific literature reports no cases of forming hydrosilicate nanotubes with a narrow distribution in outer diameter, and especially in length, during the early stages of phase formation. This is despite wide variations in the *T–P* conditions of synthesis [8–18], the use of different precursors [8–11, 16–20], and hydrothermal media of various compositions [11, 20–23]. Only after prolonged hydrothermal treatment do the outer diameters, inner diameters, and lengths of the nanotubes become uniform [22, 24–28]. Numerous additional questions arise when attempting to synthesize nanotubes of variable composition, i.e., with partial substitution of cations in the octahedral and tetrahedral sublattices, as well as when substituting OH^- anions with F^- [20, 29–42]. Even more questions are prompted by the experimentally observed effect of non-uniform radial distribution of cations within the octahedral sublattice during the synthesis of variable-composition nanotubes with the chrysotile structure [41–43]. Potentially, this effect could be explained by the energetic preference of cations of different sizes for specific localization sites, depending on the radius of curvature of the cation sublattice within the nanotube (Fig. 1) [41, 43]. However, the influence of a kinetic factor on this cation distribution cannot be ruled out either, as observed, for example, in the synthesis of variable-composition orthophosphates with the rhabdophane structure [44]. It is also possible that both of these factors contribute to this effect. A separate question concerns the reasons for the diversity in the forms of nanotubular particles with the chrysotile structure, which is particularly pronounced in the initial stages of synthesis [9, 25, 35, 38, 45, 46]. Moreover, as shown in [38], the extent of this morphological heterogeneity of nanotubes may also depend on the degree of ion substitution in $(Mg_{1-x}Ni_x)_3Si_2O_5(OH)_4$.

The analysis conducted in [11] shows that the formation mechanism can significantly influence the morphology of nanotubes with a chrysotile structure. In this regard, study [47] analyzed the impact of using pre-synthesized hydroxides of variable composition, $(Mg_{1-x}Ni_x)(OH)_2$ [48], as reagents on the formation of $(Mg_{1-x}Ni_x)_3Si_2O_5(OH)_4$ nanotubes. However, several questions regarding the specific features of the formation of magnesium-nickel hydrosilicate nanotubes with the chrysotile structure in this system remain unclear. This pertains, in particular, to the significant discrepancy between the expected and actually observed differences in the morphological parameters of $(Mg_{1-x}Ni_x)_3Si_2O_5(OH)_4$ nanotubes depending on their composition [47]. Interest in the issues surrounding the formation of nanotubes with the

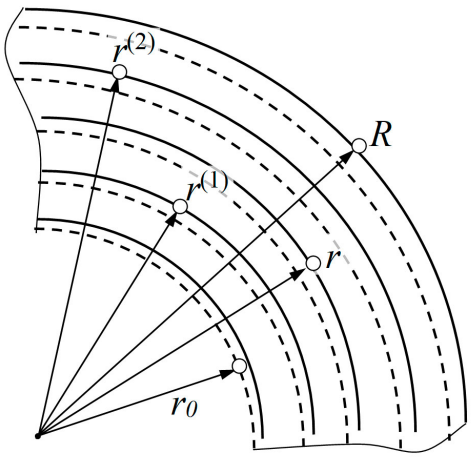

FIG. 1. Schematic diagram of a frontal section of a nanotube with a chrysotile structure. The solid circular lines represent the magnesium-nickel hydroxide layers; the dashed circular lines represent the layers based on silicon dioxide. $R = 0.5D$ and $r_0 = 0.5d$ correspond to the outer radius and diameter, and the inner radius and diameter of the nanotube, respectively; r denotes the radius of curvature of the magnesium-nickel hydroxide layer of chrysotile, with $r^1 < r^2$ representing the radii for which $x_{Ni}(r^1) < x_{Ni}(r^2)$, where $x_{Ni}(r^{\cdots})$ is the fraction of nickel ions in the corresponding layers of the compound $(Mg_{1-x}Ni_x)_3Si_2O_5(OH)_4$ [41]

chrysotile structure is sustained not only by the prospects for their application in various fields [10, 49–58] but also by the significantly lower toxicity of synthetic chrysotile compared to its natural counterpart [58].

For these reasons, there is a need to continue both computational studies and a more detailed analysis of experimental results in the field of understanding the specific features of the formation process of nanotubes with the chrysotile structure under hydrothermal conditions, particularly when using a solid solution of composition $Mg_{1-x}Ni_x(OH)_2$ as one of the reagents. This work is dedicated to this very issue.

2. Calculations

Calculations of phase relations in the (*T–P*) coordinates within the $Mg_{1-x}Ni_xO$–H_2O system were performed by analyzing the dependence of the Gibbs energy change for the dehydration reaction of $(Mg_{1-x}Ni_x)(OH)_2$ under hydrothermal conditions, leading to the formation of a $Mg_{1-x}Ni_xO$ solid solution. The calculation was carried out neglecting the contributions of the Gibbs energy of mixing of the hydroxides and oxides of variable composition to the Gibbs energy of the dehydration process. Throughout the entire investigated range of temperature and pressure changes in the system, the hydroxide and oxide phases of variable composition remain homogeneous under equilibrium conditions, i.e., they do not decompose into two hydroxide or two oxide phases. This conclusion is based on available experimental data [48] and the fact that the molar enthalpy of mixing during the formation of the $Mg_{1-x}Ni_xO$ solid solution, according to [59, 60], is either negative or $\Delta H_m^M \approx 0$. The calculations were performed using the IVTANTHERMO database and software package [61].

3. Synthesis and analysis

The starting materials used in the synthesis of nanotubes with a chrysotile structure in the $(Mg_{1-x}Ni_x)O$–SiO_2–H_2O system were hydroxides of variable composition $(Mg_{1-x}Ni_x)(OH)_2$, with a nominal composition varying within the range ($x = 0.1$, ..., 0.9), and SiO_2 in the form of silica gel (GOST 3956-76, $n = 0.73$). The hydrothermal fluid contained a solution of 5 wt.% NaOH in distilled water. The hydroxides $(Mg_{1-x}Ni_x)(OH)_2$ with nominal values varying in the interval ($x = 0.1$, ..., 0.9) were obtained by the reverse deposition method, as described in [48].

Hydrothermal treatment of the reagent mixture, calculated for the stoichiometry of $(Mg_{1-x}Ni_x)_3Si_2O_5(OH)_4$ formation, was carried out in steel autoclaves. The temperature of the hydrothermal treatment was monitored based on the furnace temperature data. Due to the thermal inertia (heating/cooling) of the thick-walled steel autoclave, the temperature of the reaction zone differs significantly from the furnace temperature. To estimate the temperature in the reaction medium during autoclave heating, a calibration curve (Fig. 2) was used, obtained by comparing the temperature in the furnace and inside the autoclave. Using identical heating conditions and the same type of autoclaves in the experiment allows for predicting the temperature in the reaction space based on the furnace temperature data for all experiments. The pressure in the reaction medium was determined using Kennedy nomograms [62] based on data on the autoclave fill factor and the temperature of the hydrothermal fluid.

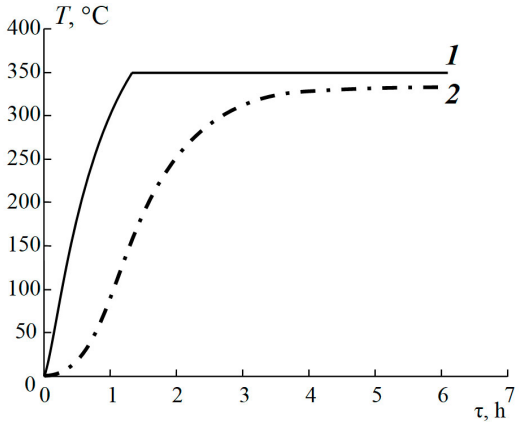

FIG. 2. Relationship between the temperature values in the furnace (1) and in the autoclave (2), according to the calibration experiment data

The hydrothermal treatment of the reagents, the post-hydrothermal operations with the resulting solid-phase products, and the analysis of the obtained samples were carried out in accordance with the methods described in [10, 47]. The dimensional parameters of the nanotubes were determined using data from transmission electron microscopy (JEM 2100-F microscope, $U = 200$ kV ($\lambda = 0.025$ Å)) and scanning electron microscopy (Hitachi S-570). To obtain statistically reliable information, random samples containing about 100 nanotubes were used in all cases, from which the average values of the outer diameter (D) and length (L) of the nanotubes were determined. The Mg/Ni ratios in the initial magnesium-nickel hydroxides and in the nanotubes were determined by EDX analysis using an attachment (Bruker Quantax 20) to a scanning electron microscope. The error in determining the Mg and Ni ratio was approximately 0.02 mole fraction.

4. Results and discussion

The results of thermodynamic calculations show that the initial mixed hydroxides $(Mg_{1-x}Ni_x)(OH)_2$, under hydrothermal treatment conditions, can dehydrate depending on their composition and temperature to form $Mg_{1-x}Ni_xO$ oxides (Fig. 3 – boundary of regions I and (II, III)). The Mg/Ni ratio in the oxide solid solution, as can be concluded from [48], will not change. This is primarily determined by the stability of $Mg_{1-x}Ni_xO$ solid solutions across the entire range of compositions down to very low temperatures, due to the fact that the molar enthalpy of mixing has negative values or is close to zero [59, 60]. Furthermore, the dehydration process can occur very quickly, as water escapes from the hydroxide nanoparticles with a layered structure through the interlayer spaces without any significant diffusion hindrance. This also contributes to preserving the Mg/Ni ratio in the oxide solid solution after dehydration of the $(Mg_{1-x}Ni_x)(OH)_2$ hydroxide.

A different situation arises during the hydration of $Mg_{1-x}Ni_xO$ under hydrothermal conditions. Despite the assumptions made based on thermodynamic calculations that, upon hydration of $Mg_{1-x}Ni_xO$ at the boundary of regions III and IV (Fig. 3), the Mg/Ni ratios in the hydroxide and oxide solid solutions should remain unchanged, the hydration reaction of $Mg_{1-x}Ni_xO$, a compound with a framework structure (periclase), will proceed significantly more slowly. In this case, on the surface of the $Mg_{1-x}Ni_xO$ crystals, for kinetic reasons, hydroxide particles enriched in magnesium ions will form first, since the driving force for the formation of such particles is significantly higher than the driving force for the formation of hydroxides enriched in nickel ions (Fig. 3). Consequently, at a certain stage of the hydration process of the $Mg_{1-x}Ni_xO$ solid solution, it can be expected that the formation reaction of "secondary" hydroxides will proceed as follows:

$$Mg_{1-x}Ni_xO + H_2O = (x_2 - x)/(x_2 - x_1)Mg_{1-x1}Ni_{x1}(OH)_2 + (x - x_1)/(x_2 - x_1)Mg_{1-x2}Ni_{x2}(OH)_2, \qquad (1)$$

where $x_2 > x > x_1$. Moreover, the values of x_1 and x_2 can vary depending on the temperature and duration of the reaction (Fig. 3 and Fig. 4). In the limiting case, x_2 can equal unity. In this situation, the hydration of oxides enriched in NiO will occur very slowly or not at all (region II, Fig. 3). Furthermore, the interaction of NiO with silicon dioxide under hydrothermal conditions to form nickel hydrosilicate is known [11, 48] to be so difficult that $NiSiO_3$ is typically used as a reagent instead of NiO to obtain nanotubular $Ni_3Si_2O_5(OH)_4$.

Given that, according to the calculations performed, throughout the entire range of *T–P* conditions of hydrothermal treatment, hydroxides $Mg_{1-x}Ni_x(OH)_2$ are stable for $x <\sim (0.55 \pm 0.05)$, taking into account the kinetic factor, one likely scenario is the hydration of the $Mg_{1-x}Ni_xO$ solid solution at the boundary of regions III and IV (Fig. 3), leading to the formation of "secondary" hydroxides via the reaction:

$$Mg_{1-x}Ni_xO + 2(1 - x)H_2O = 2(1 - x)Mg_{\sim 0.45}Ni_{\sim 0.55}(OH)_2 + (2x - \sim 1.1)NiO. \qquad (2)$$

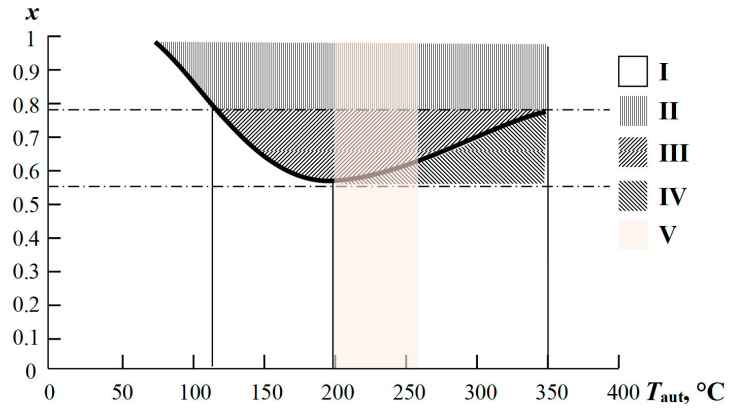

FIG. 3. Equilibrium phase state of reagent particles in the $Mg_{1-x}Ni_xO$-H_2O system according to thermodynamic calculation data, depending on the Mg/Ni ratio, temperature, and pressure in the autoclave (the pressure in the autoclave corresponding to each temperature was calculated using Kennedy nomograms [62]): I – region of existence of $(Mg_{1-x}Ni_x)(OH)_2$; II – region of formation of $Mg_{1-x}Ni_xO$ without further transformation into hydroxide; III – region of formation of $Mg_{1-x}Ni_xO$ with subsequent transformation into $(Mg_{1-x}Ni_x)(OH)_2$ upon changes in *T–P* conditions in the hydrothermal fluid; IV – region of formation of "secondary" hydroxide; V – temperature region in which the formation of chrysotile is activated [14]

As follows from (1) and (2) and is illustrated in Fig. 4, in the region of "secondary" hydration – II', for kinetic reasons, the hydroxides present will contain a smaller amount of Ni^{2+} than the original oxide. These hydroxides will be the first to interact with silicon dioxide to form nanotubes with a chrysotile structure. This conclusion is supported by the data illustrated in Fig. 3, which shows that the hydration region IV overlaps with the *T–P* region where chrysotile formation is activated.

In addition to the hydroxides in region II' (Fig. 4), one can expect to find nickel-enriched magnesium-nickel oxide solid solutions, and in the limiting case, NiO, in accordance with equation (2). During hydrothermal treatment, the components enriched in nickel oxide may either form outer layers on the surface of already formed nanotubes, initiate the formation of nanotubes significantly enriched in nickel oxide compared to the initial Mg/Ni ratio, or remain as a dispersed phase in the hydrothermal fluid due to their lower reactivity towards chrysotile formation [13]. In the latter case, they would be removed during decantation and washing of the target product precipitate.

It should be noted that the conclusions drawn from the analysis described above, within the error limits of the experiment and calculations, correlate well with the experimentally obtained data on the relationship between the composition of the initial hydroxide nanoparticles $Mg_{1-x}Ni_x(OH)_2$ and the composition of the resulting nanotubes with a chrysotile structure $(Mg_{1-y}Ni_y)_3Si_2O_5(OH)_4$ obtained using them as reagents (Fig. 5). The relationships $y(x)$ are qualitatively

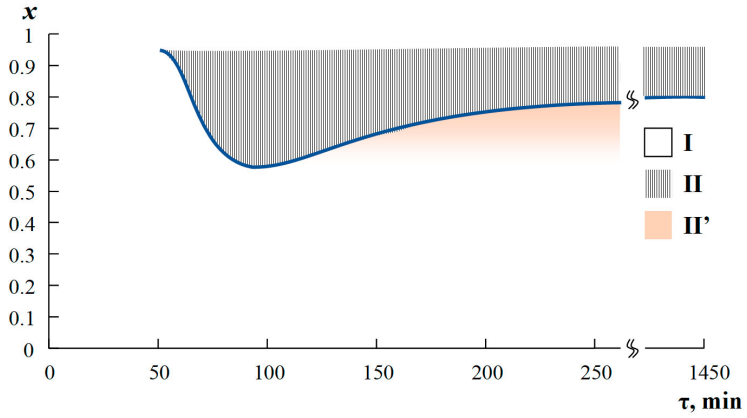

FIG. 4. Residence time of reagents in the form of hydroxide and oxide solid solutions during the hydrothermal synthesis of chrysotile for various compositions of initial hydroxides in the $Mg_{1-x}Ni_xO$–SiO_2–H_2O system. I – region of stable existence of $Mg_{1-x}Ni_x(OH)_2$; II – region of stable existence of $Mg_{1-x}Ni_xO$; II' – region of coexistence of "secondary" hydroxides and oxides in accordance with reactions (1) and (2)

divided into regions I, II, and III (Fig. 5). In terms of composition, region I (Fig. 5) corresponds to region I (Fig. 3 and Fig. 4), region II (Fig. 5) corresponds to region III (Fig. 3) and region II' (Fig. 4), and region III (Fig. 5) corresponds to region II (Fig. 3 and Fig. 4).

The characteristic feature of the dependence $y(x)$ in region II (Fig. 5) is explained by the fact that it is derived from processes preceding the formation of $(Mg_{1-y}Ni_y)_3Si_2O_5(OH)_4$ in this region: the decomposition of the hydroxide solid solution with the formation of $Mg_{1-x}Ni_xOH$ (region II – Fig. 3 and Fig. 4) and subsequent hydration (region III – Fig. 3 and region II' – Fig. 4), with the composition of the resulting "secondary" hydroxides changing according to expressions (1) and (2).

Some systematic difference in the Mg/Ni ratio between the initial reagents and the reaction products in regions I and III (Fig. 5) may be associated both with the systematic error of EDX analysis in determining the elemental composition of objects of different nature and with energetic reasons [41, 43]. When brucite-like nanoplates of $Mg_{1-x}Ni_x(OH)_2$ roll up during the formation of nanotubes with a chrysotile structure, for small values of the curvature radius – r (Fig. 1) of the brucite layer, the incorporation of Mg^{2+} ions into this layer is energetically preferable over Ni^{2+} ions [41, 43].

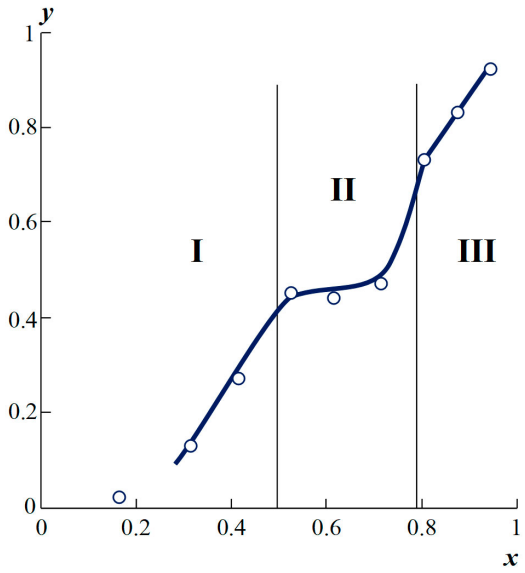

FIG. 5. Relationship between the composition of nanotubes $(Mg_{1-y}Ni_y)_3Si_2O_5(OH)_4$ and the initial hydroxides $Mg_{1-x}Ni_x(OH)_2$

Another confirmation of the concluded role of $Mg_{1-x}Ni_x(OH)_2$ dehydration and the formation of "secondary" hydroxides in the synthesis of magnesium-nickel nanotubes with a chrysotile structure is provided by the data on the dimensional parameters of the resulting nanotubes, presented in (Fig. 6). These data unequivocally show the presence of three types of characteristic dependencies of the average length (L) and outer diameter (D) of nanotubes on their composition – I, II, III (Fig. 6), the boundaries of which correlate with the boundaries of the hydroxide→oxide→hydroxide transformations for $Mg_{1-x}Ni_x(OH)_2$ solid solutions of different compositions under the conditions of their hydrothermal treatment during the experiment (Fig. 3, Fig. 4).

The sharp decrease in the size of nanotubes in region II (Fig. 6) compared to region I (Fig. 6) is explained by a sharp decrease in the formation rate of compounds with the chrysotile structure. The decrease in the formation rate of $(Mg_{1-y}Ni_y)_3Si_2O_5(OH)_4$ nanotubes for $y > (\sim 0.43)$ in region II (Fig. 6) may be related, firstly, to the fact that in region II' (Fig. 4) there is a significant proportion of oxides, which interact more slowly with SiO_2 under hydrothermal conditions than hydroxides [14]. Another reason for the sharp decrease in the nanotube growth rate in region II (Fig. 6) is the change in the Mg/Ni ratio during the formation of "secondary" hydroxides in accordance with equations (1) and (2) in region II' (Fig. 4) and, as a consequence, a decrease in the amount of nickel-enriched hydroxide reagents necessary for nanotube growth in region II (Fig. 6). The slow growth of nanotubes in region III (Fig. 6) is associated with the fact that they are formed not from hydroxides possessing a brucite structure, similar to the structure of the magnesium-nickel layer in chrysotile, but from $Mg_{1-x}Ni_xO$ oxides – region II (Fig. 3 and Fig. 4). In this case, in the absence of a reagent with a layered structure, the formation of chrysotile proceeds significantly more slowly [11–18]. It should be noted that the results obtained in this work suggest that the change in the composition of $(Mg_{1-y}Ni_y)_3Si_2O_5(OH)_4$ nanotubes along their radius (Fig. 1), with enrichment of their peripheral regions with the nickel-containing component, may be associated not only with the energetic favorability of this state, as was shown in [41], but also with kinetic factors, at least for region II (Fig. 5) of $(Mg_{1-y}Ni_y)_3Si_2O_5(OH)_4$ solid solutions, due to the specific composition of the "secondary" hydroxides formed via reactions (1) and (2) in the region (IV – Fig. 3 and II' – Fig. 4).

5. Conclusion

It has been shown that during the hydrothermal synthesis of $(Mg_{1-y}Ni_y)_3Si_2O_5(OH)_4$ nanotubes with a chrysotile structure, their composition and dimensional parameters are determined not only by the composition and prehistory of the initial reagents but also by the possibility of reagent transformation during changes in the *T–P* conditions in the reaction medium upon heating the autoclave. The thermodynamic analysis performed on the dehydration processes of $Mg_{1-x}Ni_x(OH)_2$ solid solutions and the subsequent hydration of the resulting oxide solid solutions made it possible to explain a number of effects associated with the non-monotonic dependence of the nanotube dimensional parameters and the Mg/Ni ratio in $(Mg_{1-y}Ni_y)_3Si_2O_5(OH)_4$ on the Mg/Ni ratio in the initial $Mg_{1-x}Ni_x(OH)_2$ hydroxides. The obtained results have allowed for a broader perspective on the data, which were interpreted ambiguously in some studies, concerning the influence of the composition and structure of reagents on the formation of nanotubes with a chrysotile structure.

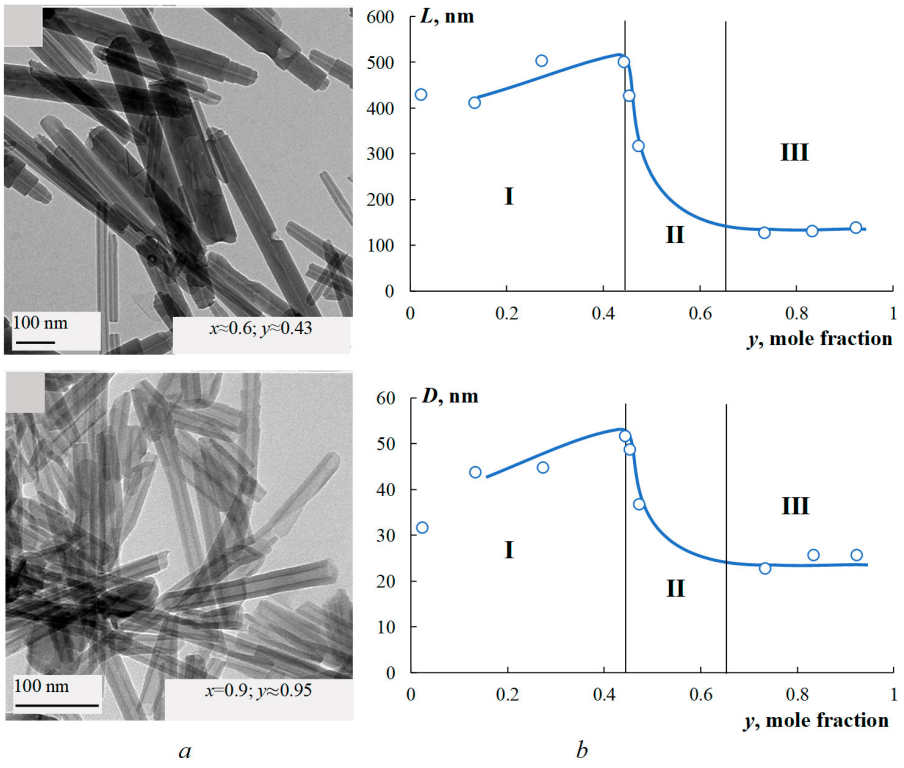

FIG. 6. Electron micrographs of nanotube samples obtained using $Mg_{1-x}Ni_x(OH)_2$ hydroxides as reagents ($x \approx 0.6$, 0.8, 0.9; $y \approx 0.44$, 0.7, 0.9 – the corresponding Ni fraction in $(Mg_{1-y}Ni_y)_3Si_2O_5(OH)_4$) – *a*; average length – *L*, and outer diameter – *D*, of $(Mg_{1-y}Ni_y)_3Si_2O_5(OH)_4$ nanotubes versus the Ni fraction – *y*, in the brucite layer of the nanotubes

References

[1] Adschiri T., Kanazawa K., Arai K., Rapid and continuous hydrothermal crystallization of metal oxide particles in supercritical water. *J. Am. Chem. Soc.*, 1992, **75** (4), P. 1019–1022.

[2] Kwon S.G., Piao Y., Park J., Angappane S., Jo Y., Hwang N.-M., Park J.-G., Hyeon T. Kinetics of monodisperse iron oxide nanocrystal formation by "heating-up" process. *J. Am. Chem. Soc.*, 2007, **129** (41), P. 12571–12584.

[3] Ivanov V.K., Kopitsa G.P., Baranchikov A.E., Grigor'ev S.V., Runov V.V., Haramusc V.M. Hydrothermal growth of ceria nanoparticles. *Russ. J. Inorg. Chem.*, 2009, **54** (12), P. 1857–1861.

[4] Kießling J., Rosenfeldt S., Schenk A.S. Size-controlled liquid phase synthesis of colloidally stable Co_3O_4 nanoparticles. *Nanoscale Adv.*, 2023, **5** (15), P. 3942–3954.

[5] Fedorov P.P., Almyasheva O.V., Alexandrov A.A., Proydakova V.Yu., Korotkova N.A., Baranovskaya V.B. Gusarov V.V. Low-temperature phase formation in the ZrO_2–In_2O_3 system. *Mendeleev Commun.*, 2025, **35** (4), P. 376–378.

[6] Almjasheva O.V., Fedorov B.A., Smirnov A.V., Gusarov V.V. Size, morphology and structure of the particles of zirconia nanopowder obtained under hydrothermal conditions. *Nanosyst: Phys, Chem, Math.*, 2010, **1** (1), P. 26–37.

[7] Sharikov F.Yu., Almjasheva O.V., Gusarov V.V. Thermal analysis of formation of ZrO_2 nanoparticles under hydrothermal conditions. *Russ. J. Inorg. Chem.*, 2006, **51** (10), P. 1538–1542.

[8] Falini G., Foresti E., Gazzano M., Gualtieri A.F., Leoni M., Lesci I.G., Roveri N. Tubular-shaped stoichiometric chrysotile nanocrystals. *Chem. A Eur. J.*, 2004, **10** (12), P. 3043–3049.

[9] Bloise A., Belluso E., Fornero E., Rinaudo C., Barrese E., Capella S., Influence of synthesis conditions on growth of Ni-doped chrysotile. *Microporous Mesoporous Mater.*, 2010, **132** (1-2), P. 239–245.

[10] L´opez-Salinas E., Toledo-Antonio J.A., Manríquez M.E., Sanchez-Cantú M., Cruz Ramos I., Hernandez-Cortez J.G., Synthesis and catalytic activity of chrysotile-type magnesium silicate nanotubes using various silicate sources. *Micropor. Mesopor. Mater.*, 2019, **274**, P. 176–182.
[11] Korytkova E.N., Maslov A.V., Pivovarova L.N., Polegotchenkova Yu.V., Povinich V.F., Gusarov V.V. Synthesis of nanotubular $Mg_3Si_2O_5(OH)_4$-$Ni_3Si_2O_5(OH)_4$ silicates at elevated temperatures and pressures. *Inorg. Mater.*, 2005, **41** (7), P. 730–736.
[12] Jancar B., Suvorov D. The influence of hydrothermal-reaction parameters on the formation of chrysotile nanotubes. *Nanotechnology*, 2006, **17** (1), P. 25–29.
[13] Sharikov F.Yu., Korytkova E.N., Gusarov V.V. Effect of the thermal prehistory of components on the hydration and crystallization of $Mg_3Si_2O_5(OH)_4$ nanotubes under hydrothermal conditions. *Glass Phys. Chem.*, 2007, **35** (5), P. 515–520.
[14] Korytkova E.N., Pivovarova L.N. Hydrothermal synthesis of nanotubes based on $(Mg,Fe,Co,Ni)_3Si_2O_5(OH)_4$ hydrosilicates. *Glass Phys. Chem.*, 2010, **36** (1), P. 53–60.
[15] Maslennikova T.P., Korytkova E.N., Gatina E.N., Pivovarova L.N. Effect of temperature on the synthesis of nanoparticles with different morphology in the system $MgO–SiO_2–TiO_2–H_2O$ under hydrothermal conditions. *Glass Phys. Chem.*, 2016, **42** (6), P. 627–630.
[16] Devouard B., Baronnet A., Van Tendeloo G., Amelinckx S. First evidence of synthetic polygonal serpentines. *Eur. J. Mineral.*, 1997, **9** (3), P. 539–546.
[17] Ueno T., Furuta Y., Koyama T., Imada T. Phase relation among serpentine, brucite and forsterite from 200 to 500 atm water pressure. *Mineral. J.*, 1991, **15** (6), P. 276–281.
[18] Krasilin A.A., Almjasheva O.V., Gusarov V.V. Effect of the structure of precursors on the formation of nanotubular magnesium hydrosilicate. *Inorg. Mater.*, 2011, **47** (10), P. 1111–1115.
[19] Lafay R., Montes-Hernandez G., Janots E., Chiriac R., Findling N., Toche F. Nucleation and growth of chrysotile nanotubes in $H_2SiO_3/MgCl_2$/NaOH medium at 90 to 300 °C. *Chemistry J.*, 2013, **19** (17), P. 5417–5424.
[20] Bloise A., Fuoco I., Apollaro C., Vespasiano G., Khrapova E., Krasilin A. Retrospective of chrysotile synthesis: From tough geoinspired process up to soft chemical design. *Applied Clay Science*, 2026, **281**, 108088.
[21] Khrapova E.K., Kozlov D.A., Krasilin A.A. Hydrothermal synthesis of hydrosilicate nanoscrolls $(Mg_{1-x}Co_x)_3Si_2O_5(OH)_4$ in a Na_2SO_3 solution. *Russ. J. Inorg. Chem.*, 2022, **67** (7), P. 839–849.
[22] Maslennikova T.P., Korytkova E.N. Influence of synthesis of physicochemical parameters on growth of $Ni_3Si_2O_5(OH)_4$ nanotubes and their filling with solutions of hydroxides and chlorides of alkaline metals. *Glass Phys. Chem.*, 2013, **39** (1), P. 67–72.
[23] Korytkova E.N., Brovkin A.S., Maslennikova T.P., Pivovarova L.N. Drozdova I.A. Influence of the Physicochemical Parameters of Synthesis on the Growth of Nanotubes of the $Mg_3Si_2O_5(OH)_4$ Composition under Hydrothermal Conditions. *Glas. Phys. Chem.*, 2011, **37** (2), P. 161–171.
[24] Chivilikhin S.A., Popov I.Yu., Svitenkov A.I., Chivilikhin D.S., Gusarov V.V. Formation and Evolution of Nanoscroll Ensembles Based on Layered-Structure Compounds. *Doklady Physics*, 2009, **54** (11), P. 491–493.
[25] Chivilikhin S.A., Popov I.Yu., Chivilikhin D.S., Gusarov V.V. Diffusion-controlled growth of a nanoscroll system. *Proceedings of Higher Educational Institutions. Physics*, 2010, **53** (3/2), P. 201–204. (In Russian)
[26] Levin A., Khrapova E., Kozlov D., Krasilin A., Gusarov V. Structure refinement, microstrains and crystallite sizes of Mg-Ni-phyllosilicate nanoscroll powders. *J. Appl. Crystallogr.*, 2022, **55** (3), P. 484–502.
[27] White R.D., Bavykin D.V., Walsh F.C. Morphological control of synthetic $Ni_3Si_2O_5(OH)_4$ nanotubes in an alkaline hydrothermal environment. *J. Mater. Chem. A*, 2013, **1** (3), P. 548–556.
[28] McDonald A., Scott B., Villemure G., Hydrothermal preparation of nanotubular particles of a 1:1 nickel phyllosilicate. *Micropor. Mesopor. Mater.*, 2009, **120** (3), P. 263–266.
[29] Thill A., Guiose B., Bacia-Verloop M., Geertsen V., Belloni L., How the diameter and structure of $(OH)_3Al_2O_3Si_xGe_{1-x}OH$ imogolite nanotubes are controlled by an adhesion versus curvature competition. *J. Phys. Chem. C*, 2012, **116** (51), P. 26841–26849.
[30] Khrapova E.K., Ivanova A.A., Kirilenko D.A., Krasilin A.A. Intermetallic compounds obtained from $Me_3Ge_2O_5(OH)_4$ (Me=Mg, Ni, Fe, Co) phyllogermanates: synthesis of single-phase precursors. *Nanosyst: Phys, Chem, Math.*, 2024, **15** (6), P. 821–836.
[31] Khrapova E.K., Ivanova A.A., Kirilenko D.A., Levin A.A., Bert N.A., Ugolkov V.L., Krasilin A.A. Phase transformations of $(Co_xMg_{1-x})_3Si_2O_5(OH)_4$ phyllosilicate nanoscrolls upon heating in Ar, O_2 and H_2 containing atmospheres. *Appl. Clay Sci.*, 2024, **250**, 107282.
[32] Khrapova, E.K., Omarov, S., Ivanova, A.A., Kirilenko, D.A., Kukushkina, Y., Krasilin, A. A. Mono- and bimetallic catalysts for the steam reforming of glycerol based on $(Co_xNi_{1-x})_3Si_2O_5(OH)_4$ phyllosilicate nanoscrolls. *Micropor. Mesopor. Mater.*, 2025, **389**, 113552.
[33] Ushio M., Saito H., Hydrothermal experiments on materials corresponding to fluor-hydroxyl chrysotile $[Mg_6Si_4O_{10}F_x(OH)_{8-x}]$. *J. Ceram. Soc. Jpn.*, 1970, **78** (11), P. 359–364.
[34] Foresti E., Hochella M. F., Kornishi H., Lesci I. G., Madden A.S., Roveri N., Xu H., Morphological and chemical/physical characterization of Fe-doped synthetic chrysotile nanotubes. *Adv. Funct. Mater.*, 2005, **15** (6), P. 1009–1016.
[35] Korytkova E.N., Pivovarova L.N., Drosdova I.A., Gusarov V.V. Hydrothermal Synthesis of Nanotubular Co-Mg Hydrosilicates with the Chrysotile Structure. *Rus. J. Gen. Chem.*, 2007, **77** (10), P. 1669–1676.
[36] Korytkova E.N., Semyashkina M.P., Maslennikova T.P., Pivovarova L.N., Al'myashev V.I., Ugolkov V.L. Synthesis and Growth of Nanotubes $Mg_3Si_2O_5(OH,F)_4$ Composition under Hydrothermal Conditions. *Glass Phys Chem.*, 2013, **39** (3), P. 294–300.
[37] Krasilin A.A., Suprun A.M., Gusarov V.V. Influence of component ratio in the compound $(Mg,Fe)_3Si_2O_5(OH)_4$ on the formation of nanotubular and platelike particles. *Russ J Appl Chem.*, 2013, **86** (11), P. 1633–1637.
[38] Krasilin A.A., Suprun A.M., Nevedomsky V.N., Gusarov V.V. Formation of conical $(Mg,Ni)_3Si_2O_5(OH)_4$ nanoscrolls. *Dokl Phys Chem.*, 2015, **460** (2), P. 42–44.
[39] Krasilin A.A., Gusarov V.V. Control over morphology of magnesium-aluminum hydrosilicate nanoscrolls. *Russ. J. Appl. Chem.*, 2015, **88** (12), P. 1928–1935.
[40] Krasilin A.A., Suprun A.M., Ubyivovk E.V., Gusarov V.V. Morphology vs. chemical composition of single Ni-doped hydrosilicate nanoscroll. *Materials Letters.*, 2016, **171**, P. 68–71.
[41] Krasilin A.A., Gusarov V.V. Redistribution of Mg and Ni cations in crystal lattice of conical nanotube with chrysotile structure. *Nanosyst: Phys, Chem, Math.*, 2017, **8** (5), P. 620–627.
[42] Krasilin A.A., Khrapova E.K., Nomine A., Ghanbaja J., Belmonte T., Gusarov V.V. Cations redistribution along the spiral of Ni-doped phyllosilicate nanoscrolls: energy modelling and STEM/EDS study. *ChemPhysChem.*, 2019, **20** (5), P. 719–726.
[43] Krasilin A.A., Gusarov V.V. Energy model of radial growth of a nanotubular crystal. *Tech. Phys. Lett.*, 2016, **42** (1), P. 55–58.
[44] Enikeeva M.O., Proskurina O.V., Gerasimov E.Yu., Gorshkova Yu.E., Naberezhnov A.A., Gusarov V.V. Gradient distribution of cations in rhabdophane $La_{0.27}Y_{0.73}PO_4 \cdot nH_2O$ nanoparticles. *Physica B.*, 2025, **696**, Art. 416623.
[45] Lafay R., Fernandez-Martinez A., Montes-Hernandez G., Auzende A.L., Poulain A. Dissolution-reprecipitation and self-assembly of serpentine nanoparticles preceding chrysotile formation: Insights into the structure of proto-serpentine *American Mineralogist*, 2016, **101** (12), P. 2666–2676.

[46] Sprynskyy M., Niedojadło, J., Buszewski, B. Structural features of natural and acids modified chrysotile nanotubes. *J. of Physics and Chemistry of Solids*, 2011, **72** (9), P. 1015–1026.
[47] Kurguzkina M.E., Maslennikova T.P., Gusarov V.V. Formation, morphology, and size parameters of nanopowders based on $Mg_3Si_2O_5(OH)_4$–$Ni_3Si_2O_5(OH)_4$ nanoscrolls. *Inorg. Mater.*, 2023, **59** (10), P. 1111–1120.
[48] Kotova M.E., Maslennikova T.P., Ugolkov V.L., Gusarov V.V. Formation, structure, composition in the dispersed state, and behavior of nanoparticles heated in the $Mg(OH)_2$–$Ni(OH)_2$ system. *Nanosyst: Phys, Chem, Math.*, 2022, **13** (5), P. 514–524.
[49] Belotitskii V.I., Fokin A.V., Kumzerov Y.A., Sysoeva A.A. Optical properties of nanowires synthesized in regular nanochannels of porous matrices. *Opt. Quantum Electron.*, 2020, **52** (4), 218.
[50] Khrapova E.K., Ugolkov V.L., Straumal E.A., Lermontov S.A., Lebedev V.A., Kozlov D.A., Krasilin A.A. Thermal behavior of Mg-Ni-phyllosilicate nanoscrolls and performance of the resulting composites in hexene-1 and acetone hydrogenation. *ChemNanoMat.*, 2020, **7** (3), P. 257–269.
[51] Bian Z., Li Z., Ashok J., Kawi S. A highly active and stable Ni–Mg phyllosilicate nanotubular catalyst for ultrahigh temperature water-gas shift reaction. *Chem. Commun.*, 2015, **51** (91), P. 16324–16326.
[52] Yang Y., Liang Q., Li J., Zhuang, He Y., Bai B., Wang X. $Ni_3Si_2O_5(OH)_4$ multi-walled nanotubes with tunable magnetic properties and their application as anode materials for lithium batteries. *Nano Res.*, 2011, **4** (9), P. 882–890.
[53] Cheng L., Zhai L., Liao W., Huang X., Niu B., Yu Sh. An Investigation on the Behaviors of Thorium(IV) Adsorption onto Chrysotile Nanotubes. *J. Environ. Chem. Eng.*, 2014, **2** (3), P. 1236–1242.
[54] Chernyaev A.V., Mikhailin N.Yu., Shamshur D.V., Kumzerov Yu.A., Fokin A.V., Kalmykov A.E., Parfen'ev R.V., Sorokin L.M., Lashkul A. Electrical and magnetic properties of Pb and In nanofilaments in asbestos near the superconducting Transition. *Phys. Solid State*, 2018, **60** (10), P. 1935–1941.
[55] Yudin V.E., Otaigbe J.U., Svetlichnyi V.M., Korytkova E.N., Almjasheva O.V., Gusarov V.V. Effects of nanofiller morphology and aspect ratio on the rheo-mechanical properties of polimide nanocomposites. *Express Polym. Lett.*, 2008, **2** (7), P. 485–493.
[56] Gubanova G.N., Sukhanova T.E., Vylegzhanina M.E., Lavrentiev V.K., Romashkova K.A., Kutin A.A., Maslennikova T.P., Kononova S.V. Analysis of the surface morphology, structure and properties of polyamidoimide nanocomposites with tubular hydrosilicates. *J. Synch. Investig.*, 2017, **11** (5), P. 1022–1032.
[57] Krasilin A.A., Khrapova E.K., Maslennikova T.P. Review: Cation Doping Approach for Nanotubular Hydrosilicates Curvature Control and Related Applications. *Crystals*, 2020, **10** (8), 654.
[58] Skuland T., Maslennikova T., Låg M., Gatina E., Serebryakova M., Trulioff A., Kudryavtsev I., Klebnikova N., Kruchinina I., Schwarze P.E., Refsnes M. Synthetic hydrosilicate nanotubes induce low pro-inflammatory and cytotoxic responses compared to natural chrysotile in lung cell cultures. *Basic Clin Pharmacol Toxicol.*, 2020, **126** (4), P. 374–388.
[59] Heath K.D., Mackrodt W.C., Saundersb V.R., Causa Mauro Calculated Enthalpies of Mixing of MnO/MgO and NiO/MgO. *J. Mater. Chem.*, 1994, **4** (6), P. 825–829.
[60] Farina A., Neto F. Thermodynamic Assessment of NiO–MgO system, September 2016 Conference: Discussion Meeting on Thermodynamics of Alloys At: Santos – Brazil 2016.
[61] Belov G.V., Iorish V.S., Yungman V.S. IVTANTHERMO for Windows - database on thermodynamic properties and related software. *CALPHAD*, 1999, **23** (2), P. 173–180.
[62] Kennedy G.C. Pressure-volume-temperature relations in water at elevated temperatures and pressures. *Am. J. Sci.*, 1950, **248** (8), P. 540–564.

Submitted 14 April 2026; accepted 15 April 2026

Information about the authors:

Oksana V. Almjasheva – NRC "Kurchatov Institute" – PNPI – IChS, Russia, Saint-Petersburg Electrotechnical University, Russia; ORCID 0000-0002-6132-4178; almjasheva@mail.ru

Maria E. Kurguzkina – NRC "Kurchatov Institute" – PNPI – IChS, Russia; ORCID 0000-0002-5817-5247; kotovamaria715@gmail.com

Victor V. Gusarov – NRC "Kurchatov Institute" – PNPI – IChS, Russia; ORCID 0000-0003-4375-6388; victor.vladimirovich.gusarov@mail.ru

Conflict of interest: the authors declare no conflict of interest.